

# A98-31649

ICAS-98-5,7,5

## PREDICTION OF FATIGUE CRACK GROWTH IN FIBER REINFORCED METAL LAMINATES

Ya-Jun Guo and Xue-Ren Wu

National Key Laboratory of Advanced Composites,  
Beijing Institute of Aeronautical Materials, 100095, China

**Abstract** Fiber reinforced metal laminates (FRMLs) is a new family of structural materials used in aircraft industry. FRMLs has excellent fatigue performance as a result of the fiber bridging. In order to predict fatigue crack growth in FRMLs, bridging traction distribution along crackline in FRMLs was first determined. Based upon the fatigue mechanisms, a theoretical model for predicting crack growth in FRMLs was developed, and applied to CCT specimens of 2/1- and 3/2-GLARE. The predicted crack growth rates from the theoretical model were in good agreement with testing results. Based on the experimental observations that crack growth in FRMLs under cyclic loading tends to reach a steady state, a phenomenological model for predicting crack growth in FRMLs was developed. This phenomenological model requires no knowledge of bridging traction and the delamination growth in FRMLs, thus greatly facilitates engineering applications. The phenomenological model has been exercised on both CCT and SENT specimens of 3/2 GLARE, very good agreement between the predicted lives and test results was found.

**Keywords:** Fiber Reinforced metal Laminates; GLARE; Bridging Traction; Fatigue; Crack Growth Rates; Delamination.

### Introduction

Fiber reinforced metal laminates (FRMLs) are a relatively new group of materials developed for the aircraft industry with improved mechanical properties and excellent fatigue performance over aluminum alloys currently being used.

FRMLs are fabricated by bonding thin aluminum alloy sheets with fiber-adhesive prepregs. The first developed FRMLs is aramid fiber reinforced aluminum sheets (with the trade-name of ARALL) laminates in the late 1970s<sup>[1]</sup>, followed by glass fiber reinforced aluminum sheets laminates (with the trade-name of GLARE)<sup>[2]</sup>. The improvement of fatigue performance stems from the bridging effect of the intact fibers in the wake of crack tip on the aluminum sheets which effectively inhibits the growth of fatigue cracks in the metal layers when subjected to cyclic loading<sup>[3]</sup>.

The fatigue crack growth rates in FRMLs are affected by fiber bridging traction and the delamination growth between the fiber-adhesive layers and the metal sheets. Fiber bridging traction and the delamination in FRMLs are interrelated during fatigue. The excellent fatigue performance of FRMLs is mainly due to the bridging of intact fibers in the wake of crack tip which restrains crack opening, thereby reducing the effective stress intensity factor actually experienced at the crack tip. Owing to such extensive shielding from fiber bridging, the fatigue crack growth rates in FRMLs exhibit no unique correlation with the nominal applied stress intensity factor range  $\Delta K$ , but is characterized by an effective stress intensity factor range  $\Delta K_{eff}^{[3]}$ , which includes the contribution of bridging traction. Bridging traction strongly depends on the delamination shape and size. In a fatigue-cracked FRMLs, the crack bridging traction is transferred from the fiber-adhesive layers to the metal sheets by the shear stress in the interfacial region. The

resulting shear deformation of the adhesive in the boundary of the delamination area allows for some crack opening displacement, decreasing the fiber bridging efficiency.

The key issue for predicting crack growth in FRMLs is how to determine the effective stress intensity factors. According to the traditional analysis based upon the fatigue damage mechanisms of FRMLs, bridging traction must be first determined, and the delamination growth characterized. Constant bridging traction along crackline assumed by Marissen<sup>[3]</sup> seems questionable because the observed delaminations in ARALL<sup>[4]</sup> and GLARE<sup>[5]</sup> during fatigue are not elliptical, and elliptical delamination is necessary for the constant bridging traction along crackline. The distribution of bridging traction along crackline therefore must be determined for a more accurate prediction of crack growth in FRMLs, which needs a fairly complex analysis, difficult for engineering applications. An analytical equation of the effective stress intensity factors is most desirable for the prediction of crack growth in FRMLs.

## 1 A Theoretical Model for Predicting Crack Growth in FRMLs Based on the Fatigue Damage Mechanism

### 1.1 Analysis of Bridging Traction Distribution in Center-Cracked FRMLs

Considering a configuration of CCT specimens of FRMLs with a saw-cut ( $2s$ ) and a current crack ( $2a$ ) subjected to remote uniform stress,  $\sigma_0$ . The fibers in the wake of the crack tip (between  $s$  and  $a$ ) are intact. The stress in the intact fibers is called bridging traction,  $\sigma_{br}$ . Delamination exists in the interface between the metal sheets and the fiber-adhesive layers on both flanks of the cracks, the shape function of delamination being  $f(x)$ . The delamination size at a saw-cut tip is  $2b_s$ .

The distribution of the bridging traction can be

determined by the displacement relation as the following:

$$\delta_{fm}(x_i) + \delta_{ad}(x_i) = u_{\infty}(x_i) - u_{br}(x_i) + \delta_{Al} \quad (1)$$

where  $\delta_{fm}$  is the extension of the bridging fibers,  $\delta_{ad}$  is the shear deformation of the adhesive in the boundary of the delaminated area,  $u_{\infty}$  and  $u_{br}$  are respectively the crack opening displacements by the remote stress and the bridging traction.  $\delta_{Al}$  is the deformation of the metal in delaminated area, which can be neglected because it is much less than the crack opening displacement.

#### *Extension of the intact fibers in the wake of crack tip*

The extension of the bridging fibers is equal to the product of the fiber strain and the delamination size :

$$\delta_{fm}(x_i) = 2\varepsilon_{br,i} l_{fm}(x_i) = \frac{2\sigma_{br,i} t_{la}}{E_{fm} t_{fm}} f(x_i) \quad (2)$$

where  $E_{fm}$  and  $t_{fm}$  are respectively Young's modulus in fiber direction and the thickness of the fiber-adhesive layers.

#### *Shear deformation of the adhesive in the boundary of the delaminated area*

The intact fibers in the wake of the crack tips inhabits the cracked sheets by the adhesive around the boundary of the delaminated area. The shear deformation of the adhesive decreases the efficiency of fiber bridging. For a double crack lap shear (DCLS) specimen with two aluminium sheets and one fiber-adhesive layer subjected to a remote stress,  $\sigma_f$  the shear deformation of the adhesive in the boundary of the delaminated area is given by<sup>[3,6]</sup>

$$\delta_{ad}^+ = \frac{2\sigma_f}{E_{la}} \sqrt{j F_{ad} F_{fm} F_{la} F_{Al}} \quad (3)$$

where  $E_{la}$  is Young's modulus of FRMLs in fiber direction,  $j$  is the interface number.  $F_{la}$ ,  $F_{Al}$ ,  $F_{fm}$ ,  $F_{ad}$  is respectively the stiffness of the laminates, the metal layers, the fiber-adhesive layers, and

the adhesive between the fibers and the metal sheets on an interface.

Equation (3) is derived for a DCLS specimen, it can also be used to calculate approximately the shear deformation of the adhesive in the boundary of the delaminated area in CCT specimens by replacing  $\sigma_f$  by the bridging traction,  $\sigma_{br}$ . In doing so, the influence of edge restraint at the crack tips and the saw-cut was neglected. The shear deformation of the adhesive in the delamination boundary in CCT specimens of FRMLs thus becomes

$$\delta_{ad}(x_i) = \frac{2\sigma_{br}(x_i)}{E_{la}} \sqrt{\frac{F_{la}F_{Al}}{jF_{ad}F_{fm}}} \quad (4)$$

*Crack opening displacement by uniform remote stress,  $\sigma_0$*

The crack opening displacement by uniform remote stress,  $\sigma_0$ , under plane stress is given by<sup>[7]</sup>

$$u_{\infty}(x_i) = \frac{4\sigma_0}{E_{la}} \sqrt{a^2 - x_i^2} \cdot \sqrt{\sec(\pi a/w)} \quad (5)$$

Equation (5) gives a good representation for isotropic materials, when applied to the anisotropic FRMLs, some discrepancy may occur (about 10 percent according to Ref.[3]).

*Crack opening displacement by bridging traction,  $\sigma_{br}$*

Because there is no closed-form solution of the crack opening displacement by a random stress acting on the crack face, a numerical method must be employed for determining the crack opening displacement by the bridging stress,  $\sigma_{br}$ . For a center crack subjected to a segment of uniform stress,  $\sigma_{br}$ , at  $x_j$ , the crack opening displacement at point  $x_i$  is given, with good approximation, by<sup>[5,8,9]</sup>

$$u_{br}(x_i) = 2 \sum_{j=1}^N \sigma_{br,j} g(x_i, x_j) L(x_j, y_j) \quad (6)$$

where  $N$  is the total number of the bar elements.  $g(x_i, x_j)$  is Green's function considering the effect of the finite plate width<sup>[8]</sup>.  $L(x_j, y_j)$  is a correction factor considering the fact that the bridging

stress does not act on the crack flank, but on the delamination contour  $(x_j, y_j)$ ,

$$L(x, y) = \sqrt{\frac{1}{2}(a^2 - x^2)} \left\{ \frac{B}{\sqrt{A}} + y^2(1+\nu) \left( \frac{BC}{A^{3/2}} - \frac{\sqrt{A+C}}{2BA} \right) \right\} \quad (7)$$

where  $\nu$  is Poisson ratio, and

$$A = (a^2 - x^2 + y^2)^2 + 4x^2y^2$$

$$B = \sqrt{a^2 - x^2 + y^2 + \sqrt{A}}$$

$$C = a^2 + x^2 + y^2$$

The distribution of bridging traction in FRMLs can be obtained by substituting eq.(2), (4), (5) and (6) into eq.(1)

$$H_{ij} \sigma_{br,j} = Q_i \quad (8)$$

with

$$H_{ij} = (P_i + D_i) \delta_{ij} + g_{ij} L_j \quad (9)$$

$$D_i = \frac{1}{E_{la}} \sqrt{\frac{F_{la}F_{Al}}{jF_{ad}F_{fm}}} \quad (10)$$

$$P_i = \frac{F_{la}}{E_{la}F_{fm}} f(x_i) \quad (11)$$

$$Q_i = \frac{2\sigma_0}{E_{la}} \sqrt{a^2 - x_i^2} \cdot \sqrt{\sec(\pi a/w)} \quad (12)$$

where  $\delta_{ij}$  is the Kronecker  $\delta$ ,  $\delta_{ij}=1$  if  $i=j$ ,  $\delta_{ij}=0$  if  $i \neq j$ .

## 1.2 Characterization of the Delamination growth in CCT Specimens of FRMLs

Delamination in FRMLs decreases the efficiency of fiber bridging, therefore the delamination growth in FRMLs under fatigue loading must be characterized. Based upon the observation of the delamination shapes in ARALL<sup>[4]</sup> and GLARE<sup>[5]</sup>, the delamination shapes in FRMLs under fatigue loading are very close to a triangle. Triangular delamination shape was thus assumed for calculating the bridging traction in CCT specimens of GLARE, and an assumption was also introduced that the delamination growth rates at saw-cut tip ( $x=s$ ) in CCT specimens of GLARE are only controlled by the bridging traction at that point ( $S_{br,s}$ ). Energy release rate was employed for characterizing the delamination growth with a

Walker-type equation,

$$\frac{db_s}{dN} = C_2 \left[ (1 - R_d)^{m_2 - 1} \Delta \sqrt{G_s} \right]^{n_2} \quad (13)$$

where  $C_2$ ,  $m_2$ ,  $n_2$  is the constants for the delamination growth in DCLS specimens, measured with a Compliance method<sup>[10]</sup>.  $R_d$  is the effective stress ratio for the delamination growth in CCT specimens<sup>[5,11]</sup>,

$$R_d = \frac{R - C^*}{1 - C^*} \quad (14)$$

with

$$C^* = \frac{F_{la} t_{fm}}{F_{Al} t_{la}} \cdot \frac{\sigma_{r, fm}}{S_{br, s}^{\max}}$$

where  $t_{la}$  and  $t_{fm}$  are the thickness of the laminates and the fiber-adhesive layers,  $\sigma_{r, fm}$  is the residual stress in the fiber-adhesive layers,  $S_{br, s}^{\max}$  is the bridging traction at the saw-cut tip corresponding to the maximum cyclic stress,  $S_{max}$  and  $R$  are respectively the maximum cyclic stress and stress ratio of CCT specimens.  $\Delta \sqrt{G_s}$  is the range of the square root of the energy release rate at the saw-cut tip, it given by<sup>[5,10,11]</sup>

$$\Delta \sqrt{G_s} = (1 - R) S_{br, s}^{\max} \frac{t_{la}}{t_{fm}} \sqrt{\omega} \quad (15)$$

with the define

$$\omega = \frac{F_{Al} t_{fm}^2}{2j F_{fm} F_{la}} \quad (16)$$

### 1.3 Analysis of Fatigue Crack Growth in FRMLs

Residual stresses exist in FRMLs because of the different thermal expansion coefficients between metal sheets and fiber-adhesive layers. Considering the effect of the residual stress on crack growth in FRMLs, the crack opening stress ( $S_{op}$ ) was introduced

$$S_{op} = - \frac{E_{la}}{E_{Al}} \sigma_{r, Al} \quad (17)$$

The crack growth rates of FRMLs can be determined by the equation of crack growth rate of the constituent metal in FRMLs, as follows:

$$\frac{da}{dN} = C_1 \left[ (1 - R_c)^{m_1 - 1} \Delta K_{eff} \right]^{n_1} \quad (18)$$

where  $\Delta K_{eff}$  is the range of the effective stress intensity factors experienced by the constituent metals at crack tips in FRMLs. Considering the fact the stress in the constituent metals of FRMLs is proportional to its Young's modulus

$$\Delta K_{eff} = \frac{E_{Al}}{E_{la}} \Delta S_{eff} \cdot f \sqrt{\pi a} \quad (19)$$

where  $f$  is the effective non-dimensional stress intensity factors

$$f = f_0 - f_{br} \quad (20)$$

where  $f_0$  and  $f_{br}$  are the stress intensity factors by unit remote stress ( $\sigma_0=1$ ) and its corresponding bridging traction,  $\sigma_{br}$  which were solved by Weight function method<sup>[5,12]</sup>.  $\Delta S_{eff}$  and  $R_c$  are respectively the effective stress range and the effective stress ratio of CCT specimens of FRMLs.

if  $S_{max} \leq S_{op}$ , there is no crack growth,

if  $S_{min} < S_{op} < S_{max}$ ,

$$\Delta S_{eff} = S_{max} - S_{op} \quad (21)$$

$$R_c = 0 \quad (22)$$

if  $S_{op} \leq S_{min}$

$$\Delta S_{eff} = S_{max} - S_{min} \quad (23)$$

$$R_c = \frac{S_{min} - S_{op}}{S_{max} - S_{op}} \quad (24)$$

Based on the above analyses, the effective stress intensity factors and the energy release rates in CCT specimens of FRMLs were determined. The effective stress intensity factors are for calculating fatigue crack growth rates based on the equation of the crack growth rate of the constituent metal of FRMLs. The energy release rates are for calculating the delamination growth rates in CCT specimens based on the equation of the delamination growth rate, obtained from DCLS specimens of FRMLs.

### 1.4 Comparison of the Predicted Crack Growth Rates by the Theoretical Model with Test Results

The present theoretical model for predicting crack growth in FRMLs was applied to CCT specimens of 2/1- and 3/2- GLARE under constant amplitude loading. The maximum cyclic stress and stress ratio for 2/1-GLARE are respectively 150MPa and 0.1, 150MPa and 0.3 for 3/2-GLARE. Figure 1 compared the predicted crack growth rates and test results.

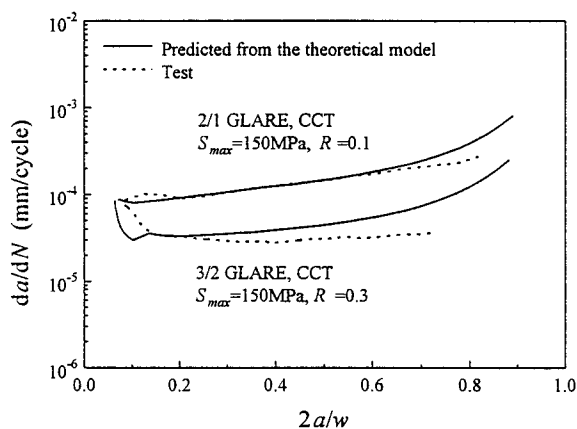


Fig.1 Comparison of predicted crack growth rates from the theoretical model and test results

It can be seen from Fig.2 that the predicted crack growth rates were in good agreement with testing results, especially when the ratios of crack length to the specimen width,  $2a/w$ , are less than 0.6. The discrepancy between the prediction and the experiment becomes larger for  $2a/w > 0.6$ . A possible explanation for the discrepancy for  $2a/w > 0.6$  is the over estimation of the width effect for FRMLs as compared to the pure metal sheets because of the restraint of the fibers. Further studies is needed to clarify this point.

## 2 A Phenomenological Model for Predicting Crack Growth in FRMLs

It can be found from the above analysis that the model for predicting crack growth in FRMLs based upon the fatigue damage mechanisms needs a fairly complex analysis for determining the distribution of the bridging traction and for

characterizing the delamination growth, difficult for engineering applications. Thus there is a growing need for a more practical model of predicting crack growth in FRMLs. The key issue for predicting fatigue crack growth rates is how to calculate the effective stress intensity factors. An analytical equation of the effective stress intensity factor is most desirable for engineering applications.

### 2.1 Characteristic of Crack Growth in GLARE

CCT specimens of 2/1-GLARE, CCT and SENT specimens of 3/2-GLARE were selected for fatigue tests. For CCT specimens, the length of the specimens is 250mm, the total width ( $w$ ) is 75mm, the saw-cut size ( $2s$ ) is 5mm and 10mm; For SENT specimens, the length of the specimens is 250mm, the width is 40mm, and the saw-cut size is 2.5mm.

The test results of the fatigue crack growth rates for the three types of specimens were shown in Fig.2; Fig.2a is for CCT specimens of 2/1-GLARE, Fig.2b and Fig.2c are respectively for CCT and SENT specimens of 3/2-GLARE. It can be seen from Fig.2 that the crack growth for both CCT and SENT specimens of 3/2-GLARE tends to a steady state after about 10 percent of fatigue life, i.e. the crack growth rates in GLARE are almost constant, even up to  $2a/w=0.9$ . For 2/1-GLARE, the crack growth rates can be regarded approximately constant during fatigue. This is an important characteristic of the fatigue behavior in FRMLs.

### 2.2 Effective Stress Intensity Factor Equation

Figure 2 shows that the crack growth rates in both the CCT and SENT specimens of GLARE are approximately constant after some cycles, such phenomena were also reported by other researchers<sup>[3,13]</sup>. This is because both the crack growth and the delamination in FRMLs depend on the bridging fibers, i.e. bridging traction, and the delamination growth in FRMLs is very

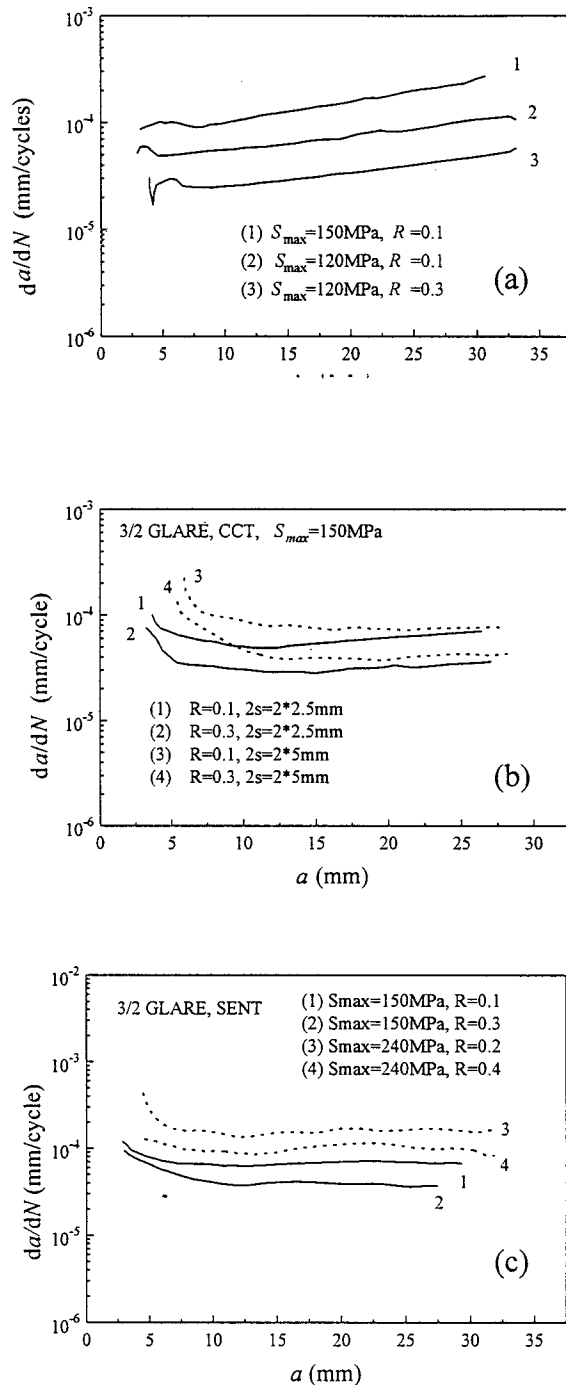


Fig.2 Test results of crack growth rates in GLARE  
 (a) for CCT specimens of 2/1-GLARE;  
 (b) for CCT specimens of 3/2-GLARE;  
 (c) for SENT specimens of 3/2-GLARE

sensitive to stress ratio, proportional to 8~10 power of  $(1-R)^{[3,10]}$ . According to the equation of

the crack growth rates, the range of the effective stress intensity factors actually experienced at the crack tip in FRMLs is also constant as a result of the constant crack growth rates during fatigue. The range of the effective stress intensity factor ( $\Delta K_{eff}$ ) can be represented by

$$\Delta K_{eff} = \Delta S \sqrt{\pi l_0} \quad (25)$$

where  $l_0$  is the equivalent crack length of GLARE.  $l_0$  should be constant during fatigue according to the characteristic of the steady crack growth in FRMLs

The range of stress intensity factor by applied stress range ( $\Delta S$ ) for the specimens with finite width is as follows:

$$\Delta K = F \cdot \Delta S \sqrt{\pi a} \quad (26)$$

where  $F$  is the configuration factor,

$$F = \sqrt{\sec(\pi a / w)} \quad (27)$$

for the CCT specimen, and

$$F = 0.265 \left(1 - \frac{a}{w}\right)^4 + \frac{0.857 + 0.265(a/w)}{(1 - a/w)^{3/2}} \quad (28)$$

for the SENT specimen<sup>[9]</sup>.

The normalized range of the effective stress intensity factor of FRMLs can be obtained by combining eq.(25) and eq.(26)

$$\frac{\Delta K_{eff}}{\Delta K} = \frac{\sqrt{l_0} / F}{\sqrt{a}} \quad (29)$$

At the beginning of crack propagation, the crack in FRMLs grows faster (see Fig.2b) because the relatively few bridging fibers can not sustain the balance of crack growth. Considering the influence of saw-cut size ( $2s$  for CCTspecimens,  $s$  for SENT specimens), a constant  $C_0$  was introduced in the denominator of eq.(29)

$$\frac{\Delta K_{eff}}{\Delta K} = \frac{\sqrt{l_0} / F}{\sqrt{a - C_0}} \quad (30)$$

the constant  $C_0$  was determined by the fact that  $\Delta K_{eff} / \Delta K$  is equal to 1 when crack length is equal to saw-cut size (i.e.,  $a = s$ , no fiber bridging)

$$C_0 = s - \frac{l_0}{F_0^2} \quad (31)$$

where  $F_0 = F|_{a=s}$ . Substituting eq.(31) into eq.(30) yields

$$\frac{\Delta K_{eff}}{\Delta K} = \frac{\sqrt{l_0} / F}{\sqrt{(a-s) + l_0 / F_0^2}} \quad (32)$$

Substituting eq.(26) into eq.(32) yields

$$\Delta K_{eff} = \frac{\sqrt{l_0}}{\sqrt{(a-s) + l_0 / F_0^2}} \cdot \Delta S \sqrt{\pi a} \quad (33)$$

Equation (33) is the equation of the effective stress intensity equation of FRMLs under cyclic loading. There is only one constant ( $l_0$ ) needed to be determined.

### 2.3 Determination of the Equivalent Crack Length ( $l_0$ ) from the Test Results of Crack Growth Rates of FRMLs

The normalized range of the effective stress intensity factors ( $\Delta K_{eff} / \Delta K$ ) in the left of eq.(32) can be determined with the testing results of the crack growth rates of FRMLs according to the equation of the crack growth rates of the constituent metal.

$$\frac{da}{dN} = C_1 [(1 - R_c)^{m_1 - 1} \Delta K]^{n_1} \quad (34)$$

where  $C_1$ ,  $m_1$ ,  $n_1$  are the crack growth constants of the constituent metal in GLARE for Walker's type equation,  $\Delta K_{eff}$  is the effective range of the stress intensity factors,  $R_c$  is the effective stress ratio considering the influence of residual stress. The effective range of the stress intensity factors can be calculated from the test results of the crack growth rates

$$\Delta K_{eff} = \frac{\sqrt[n_1]{da / dN}}{\sqrt[n_1]{C_1 (1 - R_c)^{m_1 - 1}}} \quad (35)$$

The normalized range of the effective stress intensity factors in the left of eq.(32) thus can be determined from eq.(35) and eq.(26)

$$\frac{\Delta K_{eff}}{\Delta K} = \frac{\sqrt[n_1]{da / dN}}{\sqrt[n_1]{C_1 (1 - R_c)^{m_1 - 1} \cdot (F \cdot \Delta S \sqrt{\pi a})}} \quad (36)$$

Therefore the equivalent crack length ( $l_0$ ) of FRMLs can be determined

$$l_0 = \frac{\gamma^2}{\frac{1}{F^2} - \frac{\gamma^2}{F_0^2}} \cdot (a - s) \quad (37)$$

where  $\gamma = \Delta K_{eff} / \Delta K$ , see eq.(36).

### 2.4 Characteristic of the Equivalent Crack Length ( $l_0$ ) of FRMLs

Table 1~Table 3 showed the results of the equivalent crack length of GLARE, Table 1 and Table 2 are the CCT specimens of 2/1 GLARE and 3/2 GLARE, respectively; Table 3 is for SENT specimens of 3/2 GLARE.

It can be found that the equivalent crack length ( $l_0$ ) of GLARE is independent of cyclic loading,

Table 1 Equivalent crack length ( $l_0$ ) of CCT specimens of 2/1-GLARE

Name of specimen	$S_{max}$ (MPa)	$R$	$2s$ (mm)	$l_0$ (mm)
N5-1	150	0.1	2*2.5	1.74
N5-2	150	0.3		1.68
N5-3	120	0.1		1.95
N5-4	120	0.3		1.57
N8-1	150	0.1		1.97
Mean value				1.78

Table 2 Equivalent crack length ( $l_0$ ) of CCT specimens of 3/2-GLARE

Name of specimen	$S_{max}$ (MPa)	$R$	$2s$ (mm)	$l_0$ (mm)
N2-1	150	0.1	2*2.5	1.02
N2-2		0.3		1.06
N2-3		0.1		1.05
N2-4		0.3		1.08
N3-1		0.1	2*5.0	1.05
N3-2		0.3		1.01
N3-3		0.1		1.04
N3-4		0.3		0.96
Mean value				1.03

Table 3 Equivalent crack length ( $l_0$ ) of SENT specimens of 3/2-GLARE

Name of specimen	$S_{max}$ (MPa)	$R$	$s$ (mm)	$l_0$ (mm)
N1-11	150	0.1	2.5	1.05
N1-12	150	0.3		1.10
N1-13	240	0.2		0.98
N1-14	240	0.4		1.01
Mean value				1.03

saw-cut size, crack type, specimen configuration (specimen width), and only affected by the lay-up of laminates, therefore it can be regarded as a material constant. As a result, the crack growth can be predicted with the stress intensity factor equation (i.e., eq.(33)), which is a very simple closed-formed equation. The equivalent crack length ( $l_0$ ) of FRMLs in this equation can be easily determined with only one constant amplitude fatigue test.

### 2.5 A Phenomenological Model for Predicting Crack Growth in FRMLs

Because the equivalent crack length ( $l_0$ ) of FRMLs can be regarded as a material constant, and can be determined easily with only one fatigue test, the effective stress intensity factor of FRMLs thus can be calculated analytically with eq.(33) for other specimens with different configurations and crack types under different cyclic loading; The crack growth rates in FRMLs can be calculated based on the crack growth equation of the constitute metal in FRMLs

$$\frac{da}{dN} = C_1 [(1 - R_c)^{m_1 - 1} \Delta K_{eff}]^{m_1} \quad (38)$$

According to eq.(33)

$$\Delta K_{eff} = \frac{\sqrt{l_0}}{\sqrt{(a-s) + l_0 / F_0^2}} \cdot \Delta S_{eff} \sqrt{\pi a} \quad (39)$$

where  $\Delta S_{eff}$  is the effective applied stress range considering the influence of the residual stresses in FRMLs.  $R_c$  is the effective stress ratio, see eq.(21)-(24).

### 2.6 Comparison Between the Predicted Results by the Phenomenological Model with Test Results

The predicted crack growth rates in CCT and SENT specimens of GLARE from the phenomenological model were compared with test results, shown in Fig.3.

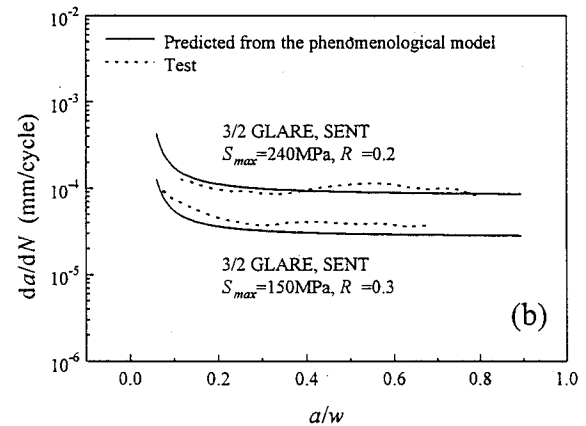
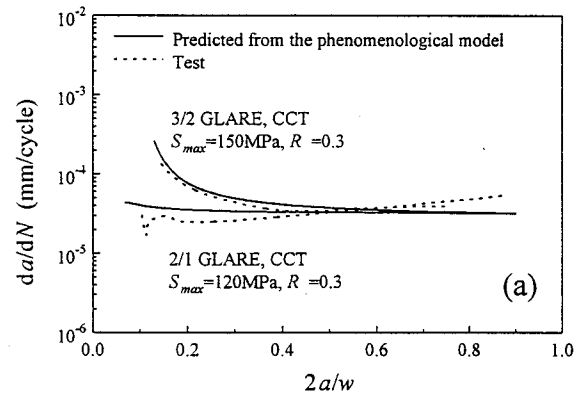


Fig.3 Comparison of predicted crack growth rates from the phenomenological model and test results  
(a) CCT specimens of 2/1- and 3/2-GLARE  
(b) SENT specimens of 3/2-GLARE

Fig.3a is for CCT specimens of 2/1- and 3/2-GLARE; Fig.3b is for SENT specimens of 3/2-GLARE. It can be seen that the predicted crack growth rates are in very good agreement with test results. The phenomenological model for predicting crack growth in FRMLs requires no knowledge of the bridging traction and the dela-



mination growth in FRMLs, and all the operations in this model are analytical, thus greatly facilitates the engineering applications.

### 3 Conclusions

Two models (a theoretical model and a phenomenological model) for predicting crack growth in fiber reinforced metal laminates (FRMLs) were developed in this paper, and applied to 2/1- and 3/2-GLARE under constant amplitude loading. The present theoretical model is based upon the fatigue damage mechanisms (i.e. fiber bridging and the delamination growth); The distribution of bridging traction in this model was determined and the delamination growth characterized. The predicted crack growth rates by the theoretical model agreed well with experimental data. The phenomenological model is developed based upon the characteristic of self-balancing growth in FRMLs, requires no knowledge of the bridging traction and the delamination growth in FRMLs, thus greatly facilitates the engineering applications. Very good agreement between the phenomenological model and test results was found.

### References

1. L. B. Vogelesang, R. Marissen and J. Schijve (1981) A New Fatigue Resistant Material: Aramid Reinforced Aluminium Laminate (ARALL). In: *17th Int. Comm. on Aeronautical Fatigue*, The Netherlands.
2. G. H. J. J. Roebroeks (1991) Towards GLARE: The Development of A Fatigue Insensitive and Damage Tolerant Aircraft Material. *Ph.D. thesis*, Delft University of Technology.
3. R. Marissen (1988) Fatigue Crack Growth in ARALL: A Hybrid Aluminium-Aramid Composite Material Crack Growth Mechanisms and Quantitative Predictions of the Crack Growth Rates. *Ph.D. thesis*, Delft University of Technology, The Netherlands.
4. J. Schijve (1993) Development of Fiber-Metal Laminates (ARALL and GLARE), New Fatigue Resistant Materials. *Fatigue '93*, 3-20.
5. Y.J.Guo (1997) Fatigue Damage and Life Prediction of Fiber Reinforced Metal Laminates (FRMLs), Ph.D. Thesis (in Chinese), Beijing Institute of Aeronautical Materials, China.
6. L. J. Hart Smith (1974) Analysis and Design of Advanced Composite Bonded Joints. *NASA CR-2218*.
7. X. R. Wu (1984) Approximate Weight Functions for Center and Edge Crack in Finite Bodies. *Engineering Fracture Mechanics*, **20** (1), 35-49.
8. J. C. Newman, Jr. (1981) A Crack-Closure Model for Predicting Fatigue Crack Growth under Aircraft Spectrum Loading. *ASTM STP 748*, 53-84.
9. H.Tada, P.C.Paris, G.R.Irwin. *The Stress Analysis of Cracks Handbook*, Second edition, Del Research Corporation, 1985
10. Y. J. Guo, X. R. Wu and Z. L. Zhang (1997) Characterization of Delamination Growth Behavior of Hybrid Bounded Laminates. *Fatigue Fract. Engng Mater. struct.*, **20** (12), 1699-1708.
11. Y.J.Guo, X.R.Wu (1998) A Model For Predicting Fatigue Crack Growth Rates In Fiber Reinforced Metal Laminates. Accepted by *Fatigue Fract. Engng Mater. struct.* for publication.
12. X. R. Wu and A. J. Carlsson (1991) *Weight Functions and Stress Intensity Factor Solutions*. Pergamon Press.
13. G.H.J.J.Roebroeks (1987) Constant Amplitude Fatigue of ARALL-2 Laminates, *Report LR-539*, Department of Aerospace Engineering, Delft University of technology.